Snapshot Wavefront Distortion Characterization Using Compressive Spectral Imagers

David J. Brady, Ashwin Wagadarikar, and Kerkil Choi
Department of Electrical and Computer Engineering, Duke University, Durham, NC 27708, USA

ABSTRACT

Atmospheric turbulence produces variations in the index of refraction of air, which leads to wavelength dependent wavefront distortions in the pupil plane. These distortions degrade the quality of images of distant objects. The wavefront distortions modify the point spread function as a function of wavelength. We have previously demonstrated the utility of coded aperture snapshot spectral imagers (CASSI) to recovering a spatio-spectral datacube characterizing the scene by measuring a snapshot, coded projection of the datacube. Here we propose the use of a CASSI for snapshot characterization of atmospheric turbulence-induced wavefront distortions and the eventual recovery of an undistorted image. Wavelength dependent phase screens are simulated following the Kolmogorov model of atmospheric turbulence and preliminary ideas for using CASSI for joint estimation of the unknown wavefront distortions and object distribution are presented.

1. INTRODUCTION

Atmospheric turbulence introduces phase aberrations that limit the resolution of incoherent imaging systems by distorting the wavefronts propagating from the object(s) being imaged. Knowledge of the phase aberrations can help to recover the object distribution. Phase diversity is an example of a multi-channel blind deconvolution scheme that has previously been used to solve this joint estimation problem [1]. In phase diversity, two or more channels with known phase differences image an object simultaneously. The process of estimating the object and the turbulence induced PSF is constrained by requiring consistency over the set of phase diverse measurements. Another multi-channel blind deconvolution scheme is wavelength diversity where the object is imaged through turbulence in multiple wavelength channels [2]. We propose to solve this joint estimation problem through the use of a snapshot spectral imager.

A spectral imager captures the power spectral density of light as a function of wavelength λ and spatial location (x, y). In other words, it acquires a three-dimensional (3D) data cube of information, (x, y; λ), about the scene being imaged. Knowledge of the spectral content at various spatial locations can be valuable in identifying the composition and structure of objects in the scene being observed by the spectral imager. It is common for most spectral imagers to acquire such a spatio-spectral data cube through temporal scanning either spectrally or spatially. Although temporal scanning is suitable for spectral imaging of a static scene, it complicates and limits the subsequent image processing and analysis for a dynamic scene due to the artifacts induced by the temporal overlap of the scanning operation of the spectral imager with dynamic changes in the scene. In contrast, Coded Aperture Snapshot Spectral Imagers (CASSI) eliminate such temporal overlap.

The rest of the paper is organized as follows. In Section 2, we review coded aperture snapshot spectral imaging and an example of a particular CASSI instrument that may be used to characterize the wavefront distortion. In Section 3, we present preliminary ideas of how a CASSI might characterize the distortion and thus potentially allow imaging of objects through atmospheric turbulence.

2. CODED APERTURE SNAPSHOT SPECTRAL IMAGING

In CASSI, the 3D spatio-spectral information about a scene of interest is encoded and acquired with one snapshot on a two-dimensional (2D) detector array. An estimate of the 3D datacube is then obtained by decoding the 2D array of measurements with numerical estimation techniques. The decoding process relies on the ideas of compressive sensing. In contrast to traditional Shannon sampling theory which requires uniform sampling of a signal at or above the Nyquist frequency for perfect reconstruction of the signal, compressive sampling has emerged as a tool that leverages the compressibility of signals in an alternate basis to the Dirac sampling basis to allow perfect or near perfect reconstruction of a signal by making a small number of projective measurements that are incoherent to the

compressive basis [3]. This leads to a large reduction in the total number of measurements required and also saves valuable sensing resources.

In encoding the 3D information into a 2D representation, a CASSI system utilizes one or more coded apertures and dispersive elements to modulate the optical field from a scene. A single-disperser CASSI (SD-CASSI) utilizes just 1 coded aperture and 1 dispersive element. Fig. 1 shows a schematic of the sensing process. Each spectral slice in the source datacube is spatially modulated by a coded aperture. This modulated datacube is then sheared with a dispersive element such as a prism. This spatially modulated and sheared datacube is then integrated along the wavelength dimension on a black and white CCD array. As a result, each pixel on the CCD measures a coded mixture of spatial and spectral information in the datacube.

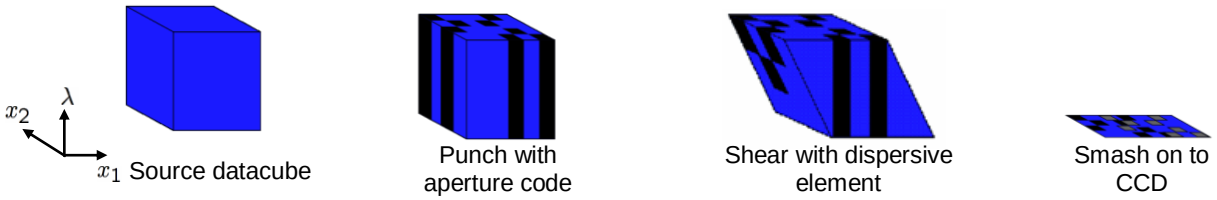

Fig. 1. Single disperser CASSI sensing process

Fig. 2 shows an example of a SD-CASSI instrument. The instrument consists of (1) an objective lens, (2) a coded aperture, (3) a bandpass filter, (4) an F/8 relay lens, (5) a double Amici prism, and (6) a monochrome charge-coupled device (CCD) detector.

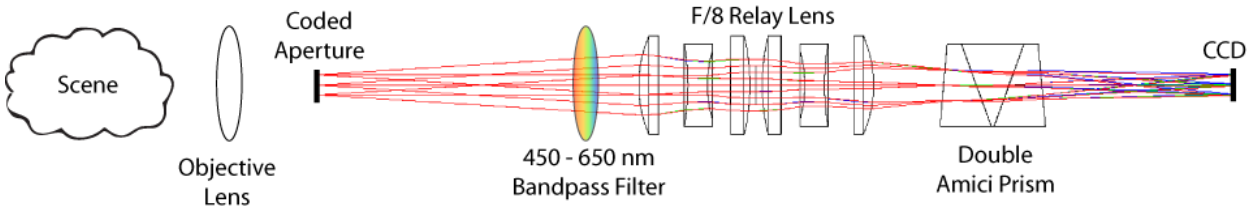

Fig.2. Schematic of the single disperser-CASSI

The objective lens images the scene on to the plane of the coded aperture. The coded aperture is lithographically patterned as a chrome coating on a quartz substrate, with an anti-reflective coating on both sides over 400-700 nm. The aperture code used in all the experiments is a random 256 x 248 element binary pattern as shown in Fig. 3, with the smallest code feature being 2 x 2 CCD pixels (19.8 um in each side). This limits the spatial size of the reconstructed data cube to 256 x 248 spatial elements.

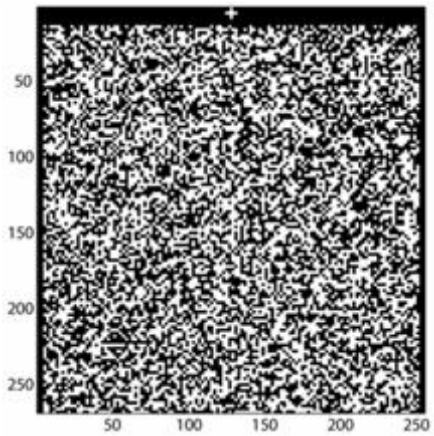

Fig.3. The aperture code used is a 256x248 binary element pattern, with the smallest feature being 2x2 detector pixels in size. The cross on the top helps to align the aperture code with the detector pixels during calibration. The bandpass filter (Semrock) limits the spectral range between 450 - 650 nm. A relay lens (Edmund Optics part C45762) relays the image from the plane of the coded aperture to the CCD. The double Amici prism is custom designed (Shanghai Optics Inc.). The angles and glass types of the prism are chosen to ensure that rays corresponding to the center wavelength of 550 nm go through the prism un-deviated, while those of adjacent wavelengths are dispersed to either side of the 550 nm rays. This property is useful because all the components of the instrument can be placed in a line on a rod-cage assembly, which makes system alignment much easier than that of our previous prototype. Furthermore, since the path lengths of all wavelengths from the prism to the CCD are similar, there is no wavelength dependent anamorphic distortion. The CCD detector is monochromatic, with 9.9 x 9.9 $(um)^2$ pixels (AVT Marlin, Allied Vision Technologies). Fig. 4 shows a 3D drawing of the single disperser prototype.

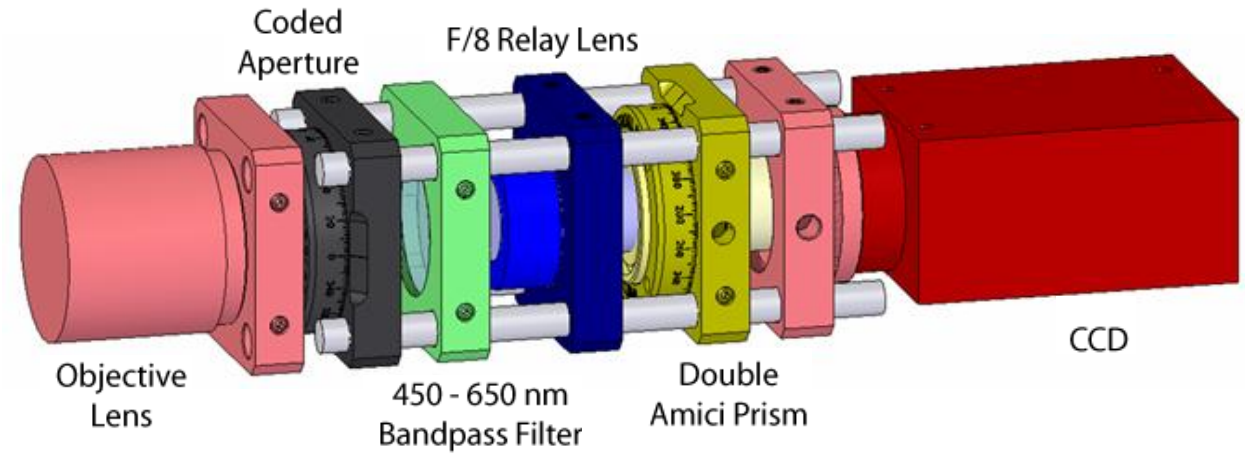

Fig. 4. Three dimensional drawing of the single disperser CASSI prototype

The detector measurements from the SD-CASSI are passed on to a numerical estimation algorithm to generate an estimate for the datacube. We can relate the detector measurements to the 3D datacube in continuous form as:

$$g = \int f(x+S(\lambda), y; \lambda) T(x+S(\lambda), y)\, d\lambda\,,$$

where f(x,y;λ) represents the spatio-spectral datacube for the scene, T(x,y) describes the aperture code function and $S(\lambda)$ describes the dispersion due to the double Amici prism. In discrete form, the measurements can be presented as:

$$g_{mn} = H_{\{mn\}\{ijk\}} f_{ijk}\,,$$

where f_{ijk} represents the discrete representation of the datacube, g_{mn} represents the 2D array of detector measurements from CASSI and H represents the system operator describing the mapping from voxels in the datacube to pixel measurements on the CASSI detector. To generate an estimate of the datacube based on the detector measurements, the numerical estimation algorithm requires a model of the system operator. This model can be generated by first calibrating the instrument. The calibration process used to produce the system-specific code involves capturing detector measurements as the input aperture of the system is uniformly illuminated with monochromatic wavelengths of light sequentially over the spectral range of the system. The system-specific code is more accurate if certain data corruptive processes are accounted for during calibration. These processes include noise on the detector array, any potential non-uniformity in the spectral intensity of the calibrating light source being coupled through a monochromator to the input aperture, and the non-uniform spectral sensitivity of the detector.

Shot noise in the detector measurement at each wavelength during calibration can be reduced averaging multiple detector measurements. Dark noise can be addressed by performing a dark background subtraction. For uniform signal-to-noise ratio (SNR) of the calibration measurements at each wavelength, the exposure time can by varied so that the mean detector counts over the image of the coded aperture on the detector is the same. The calibration light source and monochromator can be separately calibrated by measuring their combined output with a detector with a known responsivity curve such as a photodiode.

The wavelength dependent images of the aperture code obtained after averaging and background subtraction must be scaled by the non-uniform exposure time curve and the separately calibrated spectral intensity distribution function of the light source and monochromator. The end result of this process is a system-specific calibrated cube. This cube can be sampled in the spatial and/or spectral dimension(s) to produce the system-specific code, H. Fig. 5 below shows the SD-CASSI's calibrated system response to uniform illumination of the aperture code at 33 monochromatic wavelengths. As the wavelength increases, the image of the aperture code shifts due to the dispersion by the double Amici prism.

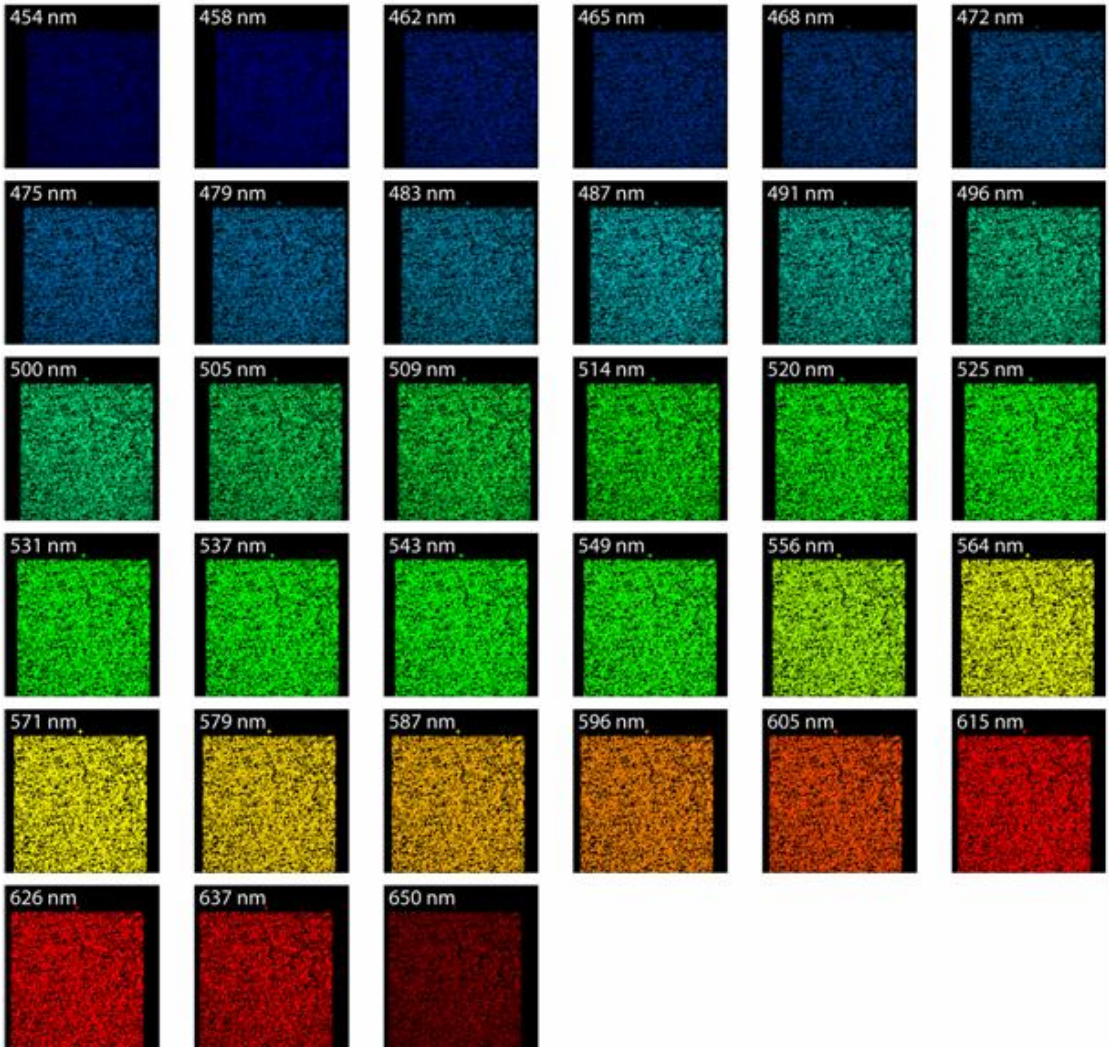

Fig. 5. Calibrated SD-CASSI system response demonstrating the instrument's response to uniform illumination of the aperture at 33 different monochromatic wavelengths.

After calibration, a datacube can be reconstructed using the Two-step Iterative Shrinkage/Thresholding (TwIST) algorithm. In the context of image reconstruction for a CASSI system, TwIST describes a datacube solution as the solution to the generalized non-linear, unconstrained minimization problem:

$$\hat{f}_{TwIST}(\tau,\Phi_{TV})=\left[\arg\min_{f}\left\{\frac{1}{2}\|g-Hf\|_2^2+\tau\Phi_{TV}(f)\right\}\right]$$

where the choices for the regularization function $\Phi_{TV}(f)$ include but are not limited to the ℓ_1 norm. We use the total variation (TV) regularizer with TwIST:

$$\Phi_{TV}(f)=\sum_{k}\sum_{i,j}\sqrt{\left[f(i+1,j,k)-f(i,j,k)\right]^2+\left[f(i,j+1,k)-f(i,j,k)\right]^2}$$

The TV term penalizes the solution candidates with higher discrete gradients horizontally and vertically. When the datacube is spatially piecewise smooth, the gradient of the image slice f_k at channel k is sparse.

Fig. 6 shows an example of a scene illuminated by fluorescent room lights. Fig. 7 shows point-wise spectra from

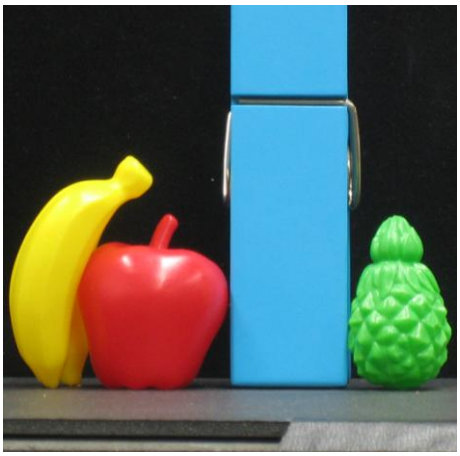

Fig. 6. Scene to be imaged by the SD-CASSI illuminated by fluorescent room lights.

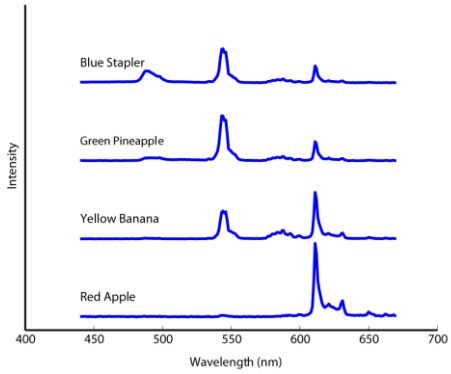

Fig. 7. Spectra from the 4 objects obtained using a point-wise, non-imaging reference spectrometer.

each of the four objects as obtained using a non-imaging reference spectrometer. Fig. 8 shows a datacube reconstruction of the scene using the TwIST algorithm. The figure shows that the spatial content of 33 spectral channels ranging from 450 to 650 nm.

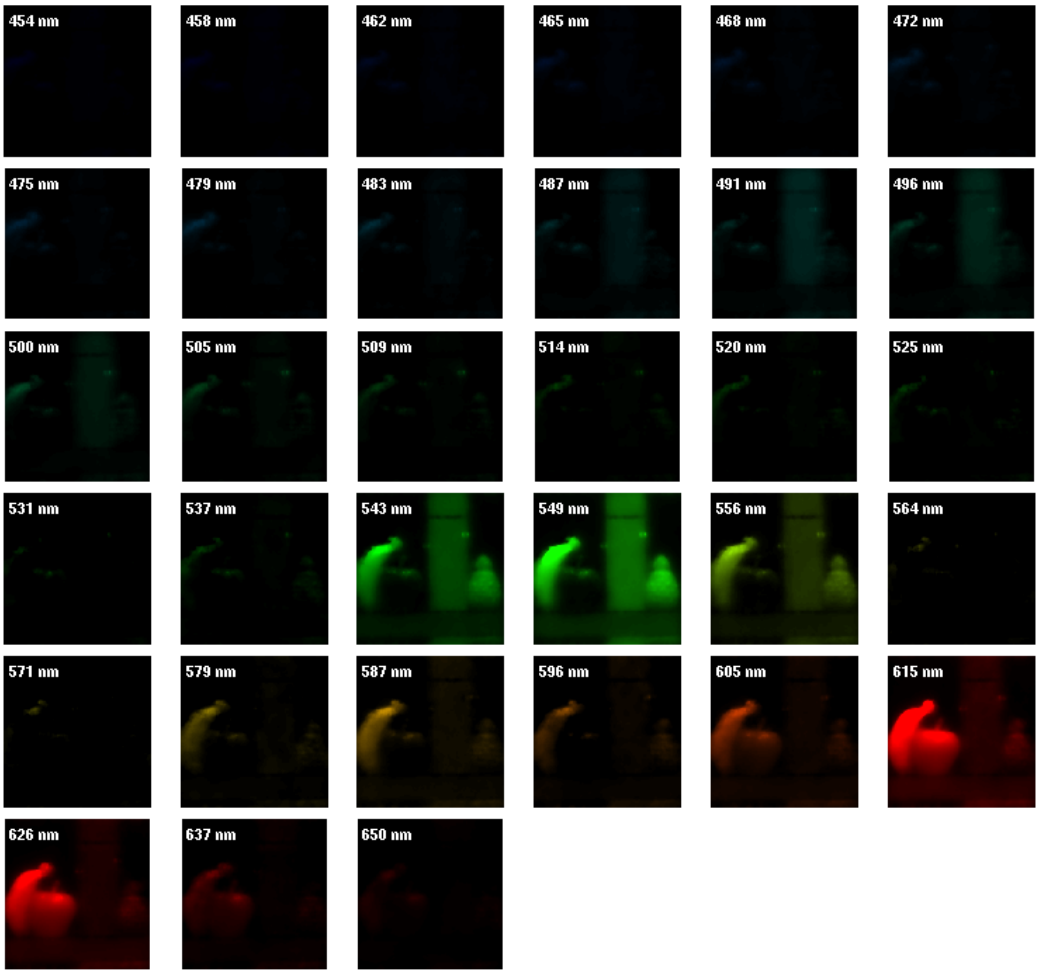

Fig. 8. The spatial content of the scene shown in 33 spectral channels ranging from 450 to 650 nm.

3. WAVEFRONT CHARACTERIZATION USING CASSI

Atmospheric turbulence can be simulated based on the assumption that it follows the Kolmogorov spectrum [5]. Fig. 9 below shows an example of an instantaneous phase screen as a function of wavelength between 450 and 650 nm generated using McGlamery's algorithm [6]. As the Figure shows, the strength of the turbulence, as dictated by the Fried parameter [7], r_0, is lower at higher wavelengths.

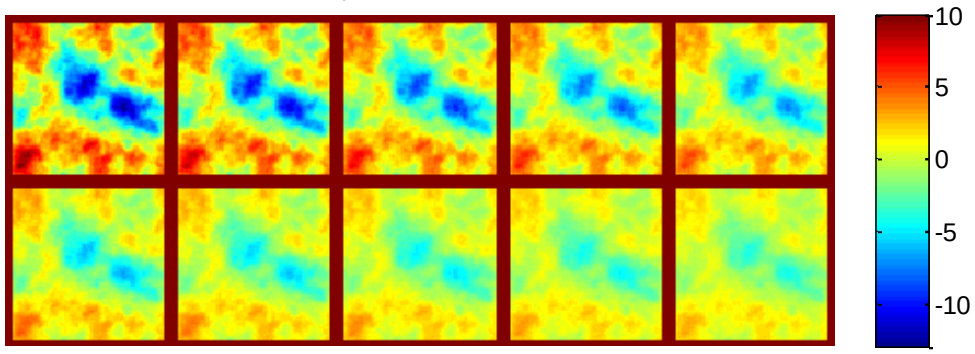

Fig. 9. Kolmogorov model phase screen spanning 450 to 650 nm, r_o=3.8 cm at 450 nm

The (incoherent) point spread function corresponding to a phase screen at a given wavelength, $\psi(u,v;\lambda)$, is given by: $h(x,y;\lambda)=\left|\Im\{e^{i\psi(u,v;\lambda)}\}\right|^2$. Fig. 10 below shows the turbulence induced PSF as a function of wavelength between 450 and 650 nm. Note that at the lower wavelengths, the PSF is significantly degraded from its ideal delta function shape.

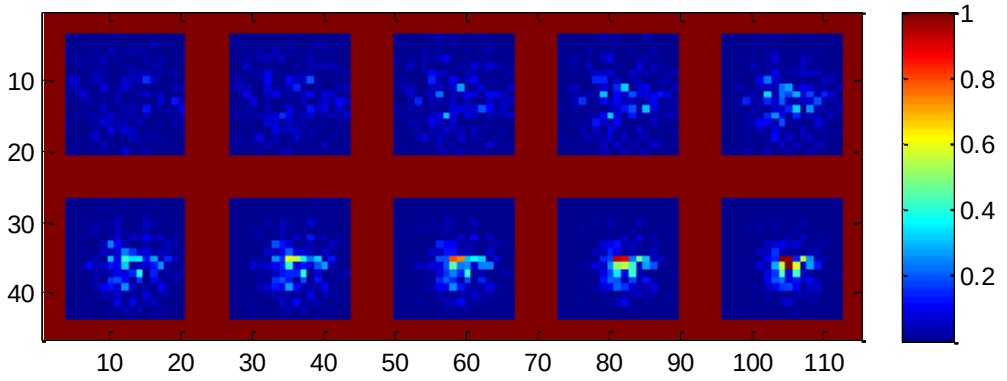

Fig. 10. Kolmogorov model PSF spanning 450 to 650 nm, r_o=3.8 cm at 450 nm

In many applications, it is reasonable to assume that the power spectral density of the object may be approximated by a constant, where the object has non-vanishing object features over a spatial bandwidth, i.e. $f(x,y;\lambda)$ has no dependence on λ and becomes $f(x,y)$ that varies only spatially. This may allow us to characterize the wavefront distortions independently of the object being reconstructed. When the object being estimated is wavelength dependent, the data captured by a CASSI can be written as $g(x,y;\lambda)=h(x,y;\lambda)*f(x,y;\lambda)$, where the data $g(x,y;\lambda)$ would result from the complicated interaction between the point spread function $h(x,y;\lambda)$ and the object $f(x,y;\lambda)$. It can be readily inferred that any slight ambiguity in the estimates of $f(x,y;\lambda)$ can cause difficulty in estimating h and vice versa.

In contrast, in the case of a wavelength independent object, the data that a CASSI captures is written as $g(x,y;\lambda)=h(x,y;\lambda)*f(x,y)$. Now, the data $g(x,y;\lambda)$ over multiple wavelengths that is captured by a CASSI may be regarded as capturing the wavelength dependent variations that are spectrally independent of $f(x,y)$. This point can better be clarified by considering the relationship in the spatial frequency domain, which becomes $\hat{g}(u,v;\lambda)=\hat{h}(u,v;\lambda)\hat{f}(u,v)$ by the convolution theorem of the Fourier transform. As this relationship indicates, the variations over λ that $\hat{g}(u,v;\lambda)$, and equivalently $g(x,y;\lambda)$, captures are the contributions by

the point spread function $\hat{h}(u,v;\lambda)$, or effectively $h(x,y;\lambda)$. This suggests that a scrutiny of the data in the spatial frequency domain $\hat{g}(u,v;\lambda)$ over wavelength would reveal information that might be good enough for the characterization of the point spread function, $h(x,y;\lambda)$. Once the PSF is characterized, it can be subsequently used, now in the spatial domain, for reconstructing the object $f(x,y;\lambda)$.

4. CONCLUSION

Wavelength diversity may be thought of as a special type of phase diversity, and many studies have demonstrated that multi-channel blind deconvolution and wavefront sensing through the diversity information are useful. Coded aperture snapshot spectral imagers (CASSI) have been used in the past to capture spatio-spectral datacubes of the scene in a snapshot. In this paper, we propose to characterize the spectrally varying point spread function induced by atmospheric turbulence using a CASSI and use this wavelength diversity information to deblur the image of a spectrally (approximately) independent object.

5. REFERENCES

1. Paxman, R.G. et al, Joint estimation of object and aberrations by using phase diversity, J. Opt. Soc. Am. A, Vol. 9, No. 7, 1072-1085, 1992.
2. Ingleby, H. and McGaughey, D.R., Real data results with wavelength-diverse blind deconvolution, Optics Letters, Vol. 30, No. 5, 489-491, 2005.
3. Healy, D. et al., Compression at the physical interface, IEEE Signal Processing Magazine, 67-71, March 2008
4. Wagadarikar, A. et al., Single disperser design for coded aperture snapshot spectral imaging, Applied Optics, Vol. 47, No. 10, B44-51, 2008.
5. Harding, C. et al., Fast simulation of a Kolmogrov phase screen, Applied Optics, Vol. 38, No. 11, 1999.
6. McGlamery, B.L., Computer simulation studies of compensation of turbulence degraded images", Proc. SPIE 74, 225-233, 1976.